Rev. Int. Contam. Ambie. 35 (Environmental Engineering of Sustainable Landscapes) 73-87, 2019
DOI: 10.20937/RICA.2019.35.esp01.08

THE FINITE ELEMENT ANALYSIS OF EN ZI TAN AQUEDUCT IN OPERATION PERIOD

Liuying SUN[1], Peng HE[1] and Zhen WANG[2]*

[1] North China University of Water Resources and Electric Power, Zhengzhou,450011, China
[2] Nanjing University of Science and Technology, Nanjing, 210094, China
*Coresponding author: 570740168@qq.com

(Received May 2018; accepted July 2018)

Key words: simple supported beam aqueduct, operation period, finite element method

ABSTRACT

As the water resources distribution in China is extremely uneven, inter-basin water transfer project has become an important part of China's water conservancy construction. As part of the the major hydraulic structure in water delivery network across rivers and transportation routes, the design and analysis on aqueduct is important. En Zi Tan Aqueduct is located in Shimen County of Hunan in China. Main content of this paper is about the finite element analysis of the aqueduct on operation period. En Zi Tan Aqueduct is designed flow is of 5.0m^3/s, longitudinal slope of 1/650, a total length of 1001m. The aqueduct is simple supported beam type, main body is reinforced concrete structure, the cross section is U-shaped and groove in each section length 13m. Top of the tank unilateral laying the bridge deck and railings in order to facilitate pedestrians. The study is using general finite element software to analize, stress and deformation changes on aqueduct body in the operation process; the water load and the earthquake influence on stress and deformation of aqueduct.

Palabras clave: acueducto soportado por una viga simple, periodo de operación, método de elementos finitos

RESUMEN

La distribución de los recursos de agua en China es extremadamente dispar, por lo que los proyectos de transferencia de agua entre cuencas se han convertido en parte importante de la infraestructura para la conservación del agua. Como parte de la estructura hidráulica principal, a través de ríos y rutas de transporte, el diseño y análisis de acueductos es importante. El acueducto En Zi Tan se localiza en el condado Shimen en Hunan, China. El contenido principal de este trabajo es acerca del análisis de elementos finitos del acueducto durante un periodo de operación. El acueducto En Zi Tan tiene un flujo designado de 5.0 m^3/s, una pendiente longitudinal de 1/650 y una longitud total de 1001 m. Se sostiene con una plataforma de viga simple, el cuerpo principal es una estructura de concreto reforzado y la sección transversal tiene forma de U con soportes cada 13 m. En la parte superior del tanque la cubierta del puente tiene barandales para facilitar el acceso. Esta investigación utiliza programas de cómputo generales de elementos finitos para analizar durante un periodo de operación los cambios por estrés y deformación en el cuerpo del acueducto; la carga de agua y la influenncia de los temblores de tierra en su estrés y deformación.

INTRODUCTIONS

The aqueduct is as an important part in the water diversion project, large number of research work has been carried out in all countries in the world (Hui 2017, Wahab and Adzmi 2017). Since 1850s, the construction of the aqueduct has been greatly developed from the design scheme and the construction technology (Jingyao 2013, Razali et al. 2017). In 70s, in order to meet the needs of large flow and large-span aqueducts, the experience of mature bridge construction was absorbed. Prestressed technology was gradually promoted and applied in aqueduct construction, which further promoted the progress of aqueduct construction (Yanhu 2012, Yasin et al. 2017). In 90s, the aqueduct played a more important role in the South to North Water Transfer Project. In the early stage, the structural mechanics method is used for the calculation of large solid structures. The accuracy of the calculation results is greatly reduced due to the excessive simplification of the solid structure. With the development of electronic computer, structure matrix analysis and finite element method, computational mechanics has been widely used, most of the complex structure can make use of the computer to complete, the calculation results can accurately reflect the actual situation of the structure, get the remarkable social and economic benefits as well as the important theoretical significance and engineering application value (Navy 2011, Kumruzzaman and Sarker 2017).

The aqueduct has a long history in our country. In ancient times, people chiseled wood for grooves and led water across the valley, that is, the oldest aqueduct. Although the aqueduct has a long history as a water conveyance building in China, the real development of the aqueduct is in modern (Guangmin et al. 2007, Yun et al. 2018). Since 1949, a large number of aqueducts have been built to solve the problem of water use in agriculture. In 50s, due to the restriction of all aspects of technology economy, most construction of the aqueduct is made of wood structure (Haut and Viviers 2006, Toum et al. 2018). Because of the lack of wood, large maintenance cost and short life, wood aqueduct is not used in this form except for a few temporary buildings. The construction of stone arch aqueduct obtains raw material locally, requires a lot of labor of stone mining, processing and construction, low technical difficulty, simple construction, low cement and steel consumption, which cater to the demands of the economy in 50 s (Zhang and Li 2011, Yasin and Usman 2017). Therefore, a considerable part of the stone arch aqueduct in many irrigation districts. In the mid 50 s, because of the development of national economic construction, reinforced concrete aqueduct increased gradually, and the construction method was mainly based on site pouring. To 1955, Heilongjiang Province, the first application of the assembly type aqueduct, after 60s, the assembly type aqueduct has been extended, due to the improvement of construction, a lot of wood and labor is saved, the project cost is reduced, the construction speed is accelerated, and more convenient in construction management and more improvement on the quality of the project. The flow rate of the aqueduct is relatively low before 70 s, and the structure form is mostly small and medium span (Elkafrawy et al. 2017, Lijie and Feng 2018). To 70 s, in order to meet the development of large irrigation areas in China, the aqueduct has changed greatly from design to construction, the water capacity of the aqueduct by several cubic meters per second to dozens of cubic meters, single span can be more than 100 meters, structure and construction develop greatly from the original assembly type to a variety of construction methods. The double crater double curved arch aqueduct built in Gaoyao County of Guangdong Province in 1975 has a span of up to 110 m (Ji 2012, Basheer et al. 2017). Guangxi Yulin Wanlong hyperbolic arch aqueduct built in 1976 span up to 126 m. The development of the prestressed technology and the successful application of the bridge have further promoted the development of the construction of the aqueduct. In the completed water supply reconstruction project "Dongshen", aqueduct is one of the selected design buildings, total length of 7.3 km, longest Jinhu aqueduct is up to 5.7 km long, designed water capacity is up to 90 m^3/s, 7-degree seismic fortification intensity, U section type, which set up a domestic precedent. In the project of South to North Water Transfer, the aqueduct plays an important role (Huang et al. 2016). South to North Water Transfer, large scale and high investment, is the largest cross basin water diversion project above the world. The main canal across the river, there are more than 1200 roads and bridges and culverts, the aqueduct as an essential item in the project interchange of water building, more reasonable and practical, economic, beautiful, safe, scientific research design and construction technology of the aqueduct, will produce huger social benefits.

As an important building of water diversion, the aqueduct has a long history, aqueduct is used to transport water across the river channels, valleys, depressions and roads, more for irrigation water, drainage, discharge, large aqueduct can also be navigable (Valeti et al. 2016). The earliest aqueducts in the world were built in the Middle East and West Asia. In more than 700 BC, Armenia already has a aqueduct. In 703 BC, the Assyrian Empire Sennarcherib ordered the construction of a 483 km long water diversion to Nineveh's aqueduct (Ji 2013). The aqueduct built on the stone wall, across the valley of sevin. The stone wall is 21 m wide, 9 m high, and about 2000000 stones are shared. There are 5 small bridge arches under the aqueduct, allowing the stream to flow. Many cities in ancient Greece built good aqueducts, but the ancient Romans were the most serious and regarded the water supply system as an important part of public health facilities (Ji 2013). Rome the first water supply aqueduct is a shelter aqueduct built in 312 BC; Alexander aqueduct is the tenth and also the last one is built in 226 ad; the longest and most spectacular was built in 114 BC Malaysia aqueduct, although the water away from Rome is only 37 km, but the aqueduct itself up to 92 km (Zhang et al. 2011). This is because the aqueduct should keep a certain slope and build it through the terrain.

China's aqueduct has a history of origin and circulation. The oldest aqueduct in China was built in the Western Han Dynasty for more than 2000 years, but there was no complete reservation. The early construction of the aqueduct are almost wood structures (Trivedi et al. 2018, Yang et al. 2017, Wang et al. 2018, Strzelecki and Sempruch 2016). In 1930s, a reinforced concrete aqueduct -appeared. In the mid twentieth Century of China, the backwardness of water conservancy facilities had a direct impact on the development of rural areas. In order to get rid of this dilemma, irrigation and irrigation has become a prominent livelihood project. As a kind of water conservancy facilities, aqueduct is beginning to build in large-scale in the country in this context, it has witnessed the development of modern agriculture and water conservancy of China transforms (Erdman et al. 2017, Khan et al. 2017). After 60s, with the development of large-scale irrigation projects, various light structure aqueduct, large span arch aqueduct is widely used. The aqueduct is now used in many water conservancy projects and water diversion projects, and more characteristic new types of aqueducts and modern aqueducts have been created.

Due to the section size and structure weight, large flow and long span aqueducts is difficult for lifting and installation without mechanical equipment with high lifting capacity and installation accuracy, which leads to various construction methods. Such as prefabricated pushing method, site pouring method, semi - field semi - assembly method, etc. Nowadays, the aqueduct construction attaches great importance to the introduction of advanced technology. The advanced thinking template of the bridge erection machine in bridge construction is a reference to the aqueduct construction, further reducing the difficulty of construction and saving engineering cost. Aqueduct structure development is also varied, rectangular aqueduct, U aqueduct, elliptical aqueduct and circular aqueduct, the best form of structure can be determined according to different engineering needs and characteristics.

GENERAL SITUATION OF ENGINEERING

The En Zi Tan aqueduct is located in Shimenn County, Hunan,China, with a design flow of 5.0m3/s, a longitudinal slope of 1/650, and a full length of 1,001 m. This aqueduct is a simply supported beam aqueduct, reinforced concrete structure. The section is U type. Each slot is 13 m long, and bridge deck and railing are laid on the side of the top of the trough to facilitate pedestrians. The ends of the grooves are placed on a single row or two rows of shelves of reinforced concrete, with a single row of shelves below 32 m, and a double row of shelves for those above 32 m. The density of the concrete is 2,500 kg/m^3, the elastic modulus is 3E10 MPa, the Poisson's ratio is 0.167, the steel density is 7,800 kg/m^3, the elastic modulus is 2E11 MPa, and the Poisson's ratio is 0.3, as shown in **Fig. 1**.

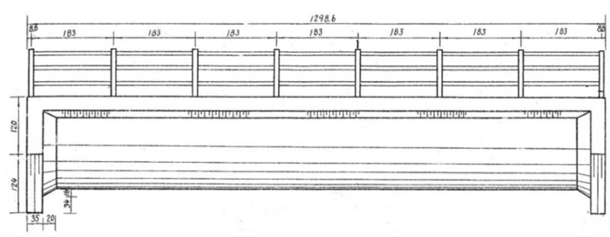

Fig. 1. The vertical view of the aqueduct

Construction method: in addition to a part of the high shelf for cast-in-place, all for prefabricated hoisting. Subsection pouring for all prefabricated high row frames, the reinforcement should be rapidly welded after lifting, and the second phase concrete should be poured to ensure the integrity of the bent column.

Working conditions

During the operation of the aqueduct structure, the following conditions should be taken into consideration:

Working condition 1: structure self-weight;

Working condition 2: structure self-weight + Half trough of water level;

Working condition 3: structure self-weight + designed water level;

Working condition 4: structure weight + bank full water;

Working condition 5: structure self-weight + designed water level + earthquake influence;

Channel body model and unit introduction

This course is designed to be a U type aqueduct, which is only modeled and analyzed for the 12m aqueduct body. The model is shown in **Fig. 2**. Before the mesh is divided, the material attributes are defined before, and when the grid is divided, the hexahedron is used as much as possible. Unit division is as shown in **Fig. 3**.

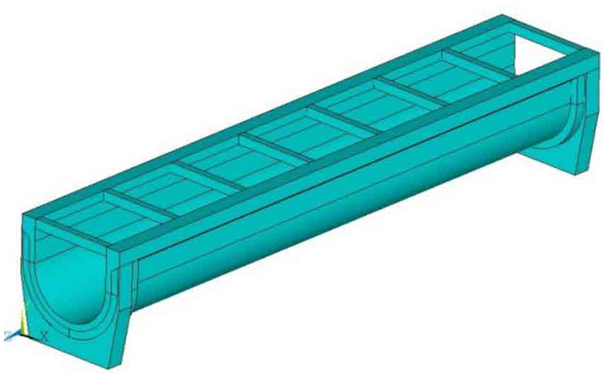

Fig. 2. Geometric model of aqueduct

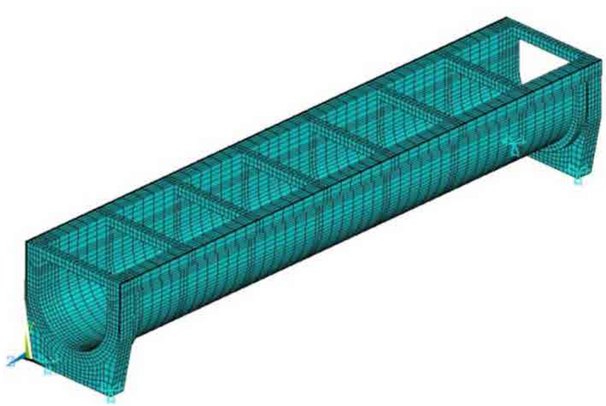

Fig. 3. Unit division

The units used in this model are Solid45, MPC184 and SHELL63 units, as is shown in **Fig. 4**, **Fig. 5**.

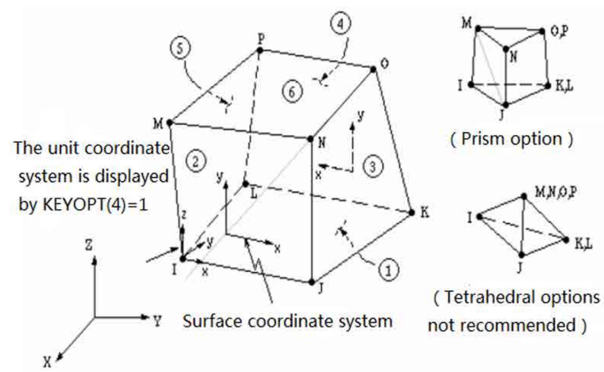

Fig. 4. Solid45 Element geometric model

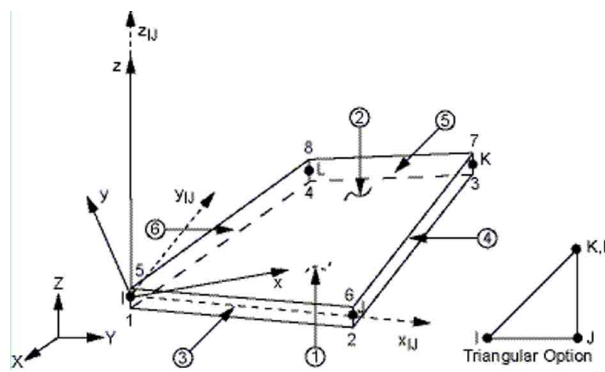

Fig. 5. SHELL63 Element geometric model

Computing paths

In order to facilitate the analysis of the variation of the displacement of large aqueducts under different working conditions along a certain line, there are 3 paths to analyze the aqueduct structure. The specific division of the 3 paths is shown in **Fig. 6**. In addition, the stress of path 1 and path 3 along the direction of Y axis is emphatically analyzed in the study, because the force on the slot end and the cross section is special.

STRUCTURAL STATIC CALCULATION RESULTS AND ANALYSIS

Working condition 1

The analysis of the stress calculation results above is as follows:

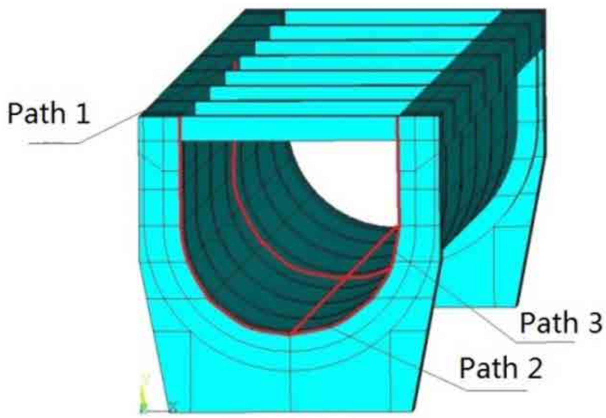

Fig. 6. Paths diagram

The stress results above all meet the strength requirements of C30 concrete. The maximum positive stress in the direction of X is 0.746731Mpa, the maximum positive stress in the direction of Y is 0.764932Mpa, and the maximum positive stress in the direction of Z is 0.716912Mpa. The stress in the y direction is the max (as is shown in **Fig 7**) and should be taken into account in the design. The maximum shear stress ofτ_{xy} is 0.508350Mpa, and the maximum shear stress is 0.680991Mpa, and the maximum shear stress is 0.228805Mpa. τ_{xz} is negligible. It can be seen from the comparison of the normal stress and the shear stress that the positive stress is larger. Therefore, the effect of the positive stress should be taken into consideration in the design. It can be seen from the results that the force of the trough end is more complex and should be paid attention.

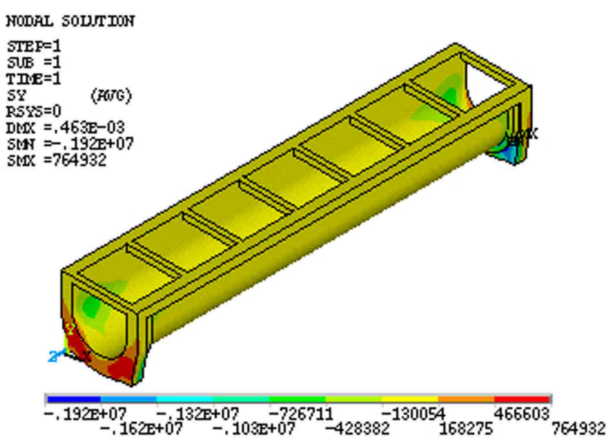

Fig. 7. The main stress of Y direction in working condition 1 (unit: pa)

The analysis of the results of the displacement above is as follows:

From the above results it can be seen that the displacement of each direction is within the allowable range and meets the requirements of the engineering design. The maximum displacement of the direction is 0.164E-04m, the maximum displacement of the Y direction is 0.463E-03m (as is shown in **Fig. 8**), the maximum displacement of the Z direction is 0.981E-04m, and the maximum total displacement is 0.463E-03m.

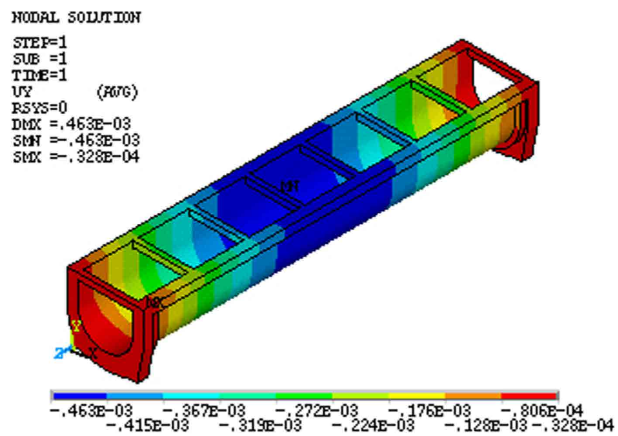

Fig. 8. The main displacement of Y direction in working condition 1 (unit: m)

Working condition 2

The analysis of the stress calculation results above is as follows:

The stress results above all meet the strength requirements of C30 concrete. The maximum positive stress in the direction of X is 1.17Mpa, the maximum positive stress in the direction of Y is 1.19Mpa, and the maximum positive stress in the direction of Z is 1.12Mpa. The stress in y direction of the three direction is the max (as is shown in **Fig. 9**) and should be taken into account in the design. The maximum shear stress ofτ_{xy} is 0.748429Mpa, and the maximum shear stress ofτ_{yz} is 1.03Mpa, and the maximum shear stress ofτ_{xz} is 0.345749Mpa. τ_{xz} is negligible. Same as the working condition one, compared with the normal stress and the shear stress, it can be seen that the positive stress is larger. Therefore, the effect of the positive stress should be taken into consideration in the design. As the similar condition one, it can be seen from the results, the maximum stress generally occurs in the groove, especially the lower groove prone, it is easier to form stress concentration.

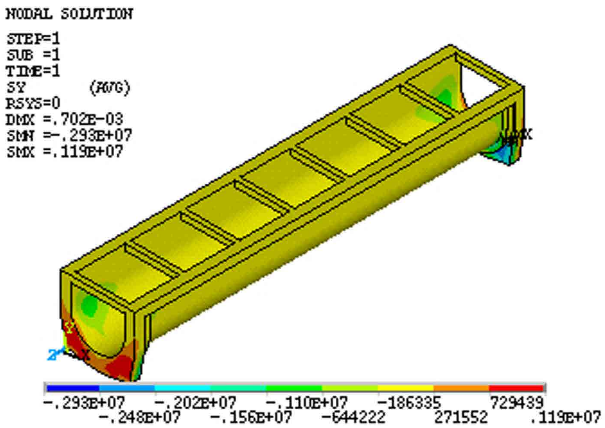

Fig. 9. The main stress of Y direction in working condition 2 (unit: pa)

The analysis of the results of the displacement above is as follows:

From the results above, it can be seen that the displacement of each direction is within the allowable range and meets the requirements of the engineering design. The maximum displacement of the direction is 0.223E-04m, the maximum displacement of the Y direction is 0.702E-03m (as is shown in **Fig. 10**), the maximum displacement of the Z direction is 0.152E-03m, and the maximum total displacement is 0.702E-03m. From the results above, it can be seen that the displacement of the cross section in the middle of the trough is large, and easier to be danger and should pay more attention to.

Working condition 3

The analysis of the results of the displacement above is as follows:

From the results above, it can be seen that the displacement of each direction is within the allowable range and meets the requirements of the engineering design. The maximum displacement of the direction is 0.480E-04m, the maximum displacement of the Y direction is 0.980E-03 (as is shown in **Fig. 12**) m, the maximum displacement of the Z direction is 0.212E-03m, and the maximum total displacement is 0.982E-03m.

Working condition 4

The analysis of the stress calculation results above is as follows:

The stress results above all meet the strength requirements of C30 concrete. The maximum positive stress in the direction of X is 1.56Mpa, the maximum positive stress in the direction of Y is 1.65Mpa, and the maximum positive stress in the direction of Z is 1.51Mpa. The stress in y direction of the three direction is the max (as is shown in **Fig. 11**) and should be taken into account in the design. The maximum shear stress of τ_{xy} is 0.974309Mpa, and the maximum shear stress of τ_{yz} is 1.46Mpa, and the maximum shear stress of τ_{xz} is 0.499556Mpa. τ_{xy} is negligible. Same as the working condition one and two, compared with the normal stress and the shear stress, it can be seen that the positive stress is larger. Therefore, the effect of the positive stress should be taken into consideration in the design. As the similar condition one and two, it can be seen from the results, the maximum stress generally occurs in the groove,

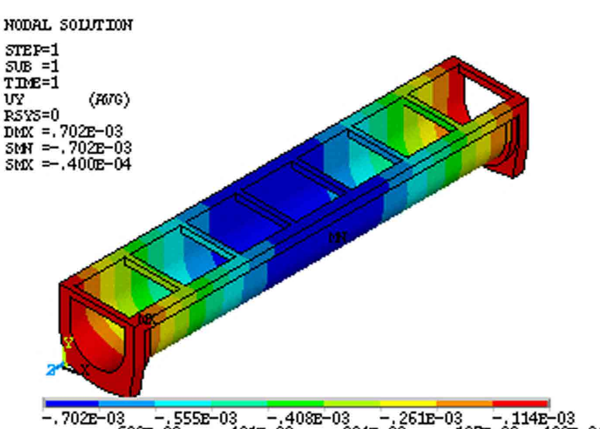

Fig. 10. The main displacement of Y direction in working condition 2 (unit: m)

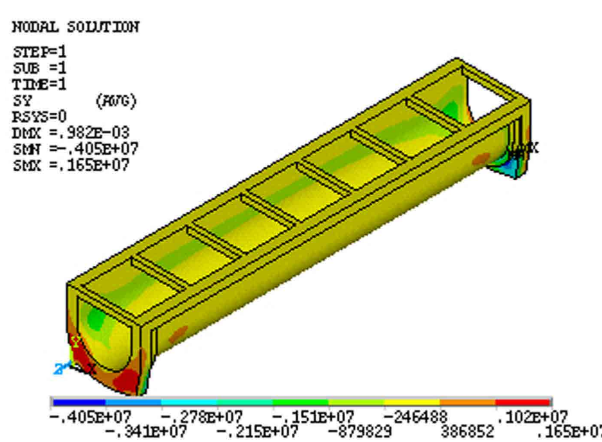

Fig. 11. The main stress of Y direction in working condition 3 (unit: pa)

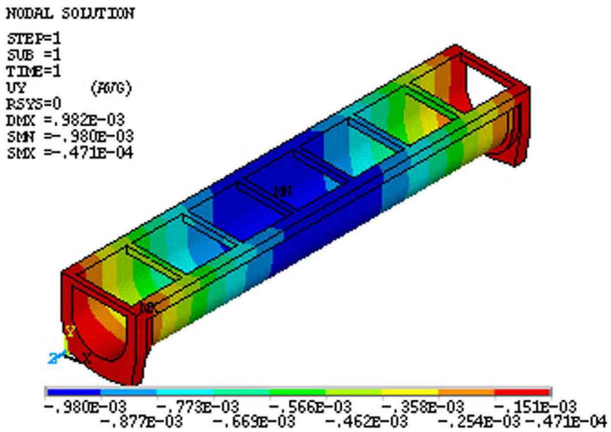

Fig. 12. The main displacement of Y direction in working condition 3 (unit: m)

especially the lower groove prone, it is easier to form stress concentration.

The analysis of the stress calculation results above is as follows:

The stress results above all meet the strength requirements of C30 concrete. The maximum positive stress in the direction of X is 1.67 Mpa, the maximum positive stress in the direction of Y is 1.79 Mpa, and the maximum positive stress in the direction of Z is 1.62 Mpa. The stress in y direction of the three direction is the max (as is shown in **Fig. 13**) and should be taken into account in the design. The maximum shear stress ofτ_{xy} is 1.04 Mpa, and the maximum shear stress ofτ_{yz} is 1.59 Mpa, and the maximum shear stress ofτ_{xz} is 0.546, 883 Mpa. τ_{xz} is negligible. Same as the working condition one, two, three, compared with the normal stress and the shear stress, it can

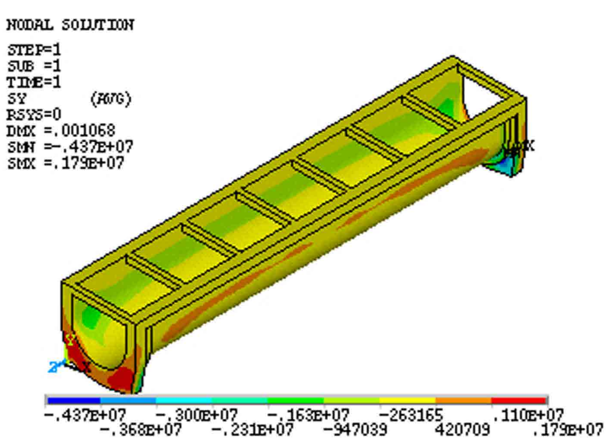

Fig. 13. The main stress of Y direction in working condition 4 (unit: pa)

be seen that the positive stress is larger. Therefore, the effect of the positive stress should be taken into consideration in the design. As the similar condition one, two, three, it can be seen from the results, more attention should be paid to the complicated force at the end of the slot.

The analysis of the results of the displacement above is as follows:

From the results above, it can be seen that the displacement of each direction is within the allowable range and meets the requirements of the engineering design. The maximum displacement of the direction is 0.575E-04m, the maximum displacement of the Y direction is 1.067E-03m (as is shown in **Fig. 14**), the maximum displacement of the Z direction is 0.231E-03m, and the maximum total displacement is 1.068E-03m.

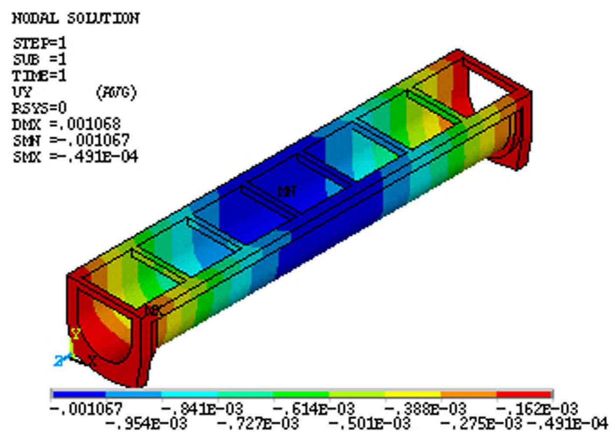

Fig. 14. The main displacement of Y direction in working condition 4 (unit: m)

Working condition 5

The analysis of the stress calculation results above is as follows:

The stress results above all meet the strength requirements of C30 concrete. The maximum positive stress in the direction of X is 1.26Mpa, the maximum positive stress in the direction of Y is 1.09Mpa, and the maximum positive stress in the direction of Z is 0.826975Mpa. The stress in x direction of the three direction is the max (as is shown in **Fig. 15**) and should be taken into account in the design. The maximum shear stress of τ_{xy} is 0.351196Mpa, and the maximum shear stress of τ_{yz} is 0.931280Mpa, and the maximum shear stress of τ_{xz} is 0.3296Mpa. τ_{xy}, τ_{xz} is negligible. Same as the working condition one, two, three, four, compared with the normal stress and the shear stress, it can be seen that the positive stress

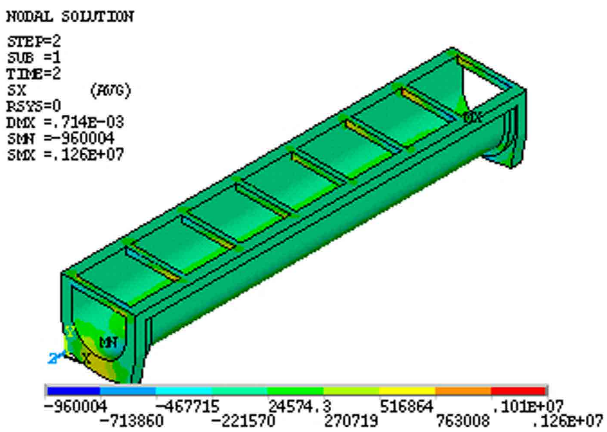

Fig. 15. The main stress of X direction in working condition 5 (unit: pa)

is larger. Therefore, the effect of the positive stress should be taken into consideration in the design. As the similar condition one, two, three, four, it can be seen from the results, the maximum stress generally occurs in the groove, especially the lower groove prone, it is easier to form stress concentration.

The analysis of the results of the displacement above is as follows:

From the results above, it can be seen that the displacement of each direction is within the allowable range and meets the requirements of the engineering design. The maximum displacement of the direction is 0.64E-05m, the maximum displacement of the Y direction is 0.149E-05m, the maximum displacement of the Z direction is 0.129E-03m (as is shown in **Fig. 16**), and the maximum total displacement is 0.714E-03m.

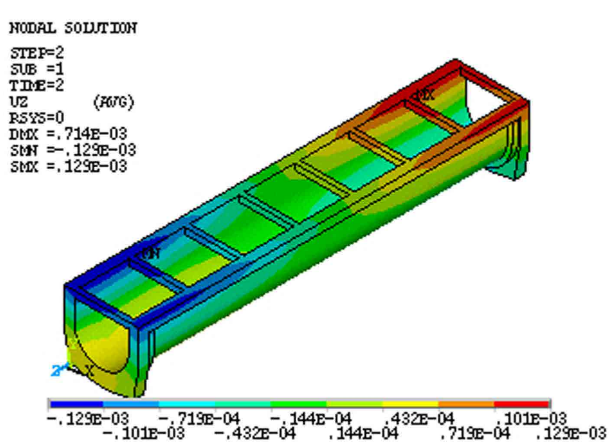

Fig. 16. The main displacement of Z direction in working condition 5 (unit: m)

ANALYSIS OF STRESS AND DISPLACEMENT OF THREE PATHS

From the above five stress calculations, we can see that the normal stress in the Y direction of the mid span section is large, so the normal stress in the Y direction of the mid span cross section is calculated and analyzed. In addition, from the above calculation of the displacement of the five working conditions, we can see that the displacement of the Y direction is large, so we focus on the calculation and analysis of the Y direction displacement and the Y direction displacement of the groove.

Path 1

Results and analysis of stress calculation in Y direction in path 1

The analysis of the above stress calculation results is as follows:

The stress results above all meet the strength requirements of C30 concrete. From the stress results above, it can be seen that there is a catastrophic surface between the tensile stress and the compressive stress. Moreover, the upper part is pressed, and the lower part is pulled. The calculation results can guide the configuration of the steel bar. For working condition five, when there are earthquakes, the stress distribution in horizontal direction is different from the first four working conditions, emphasis should be placed on the analysis, as shown in **Fig. 17**.

Results and analysis of Y direction displacement calculation in path 1

The analysis of the stress calculation results above is as follows:

The displacement results above meet the requirements of the hydraulic design specification. We can see that the condition one, three, four, the distribution of displacement is roughly the same, this is because only the aqueduct gravity is considered, or force on aqueduct relatively continuous in the designed water level and bank full water situation. On condition two and half grooves, the force in the upper and lower parts of the aqueduct is discontinuous, as is showed in the diagram. The working condition five is affected by the horizontal seismic load, as shown in **Fig. 18**.

Path 2

Results and analysis of the calculation of Y direction displacement in path 2

The analysis of the Y direction displacement of the whole aqueduct is helpful to understand the

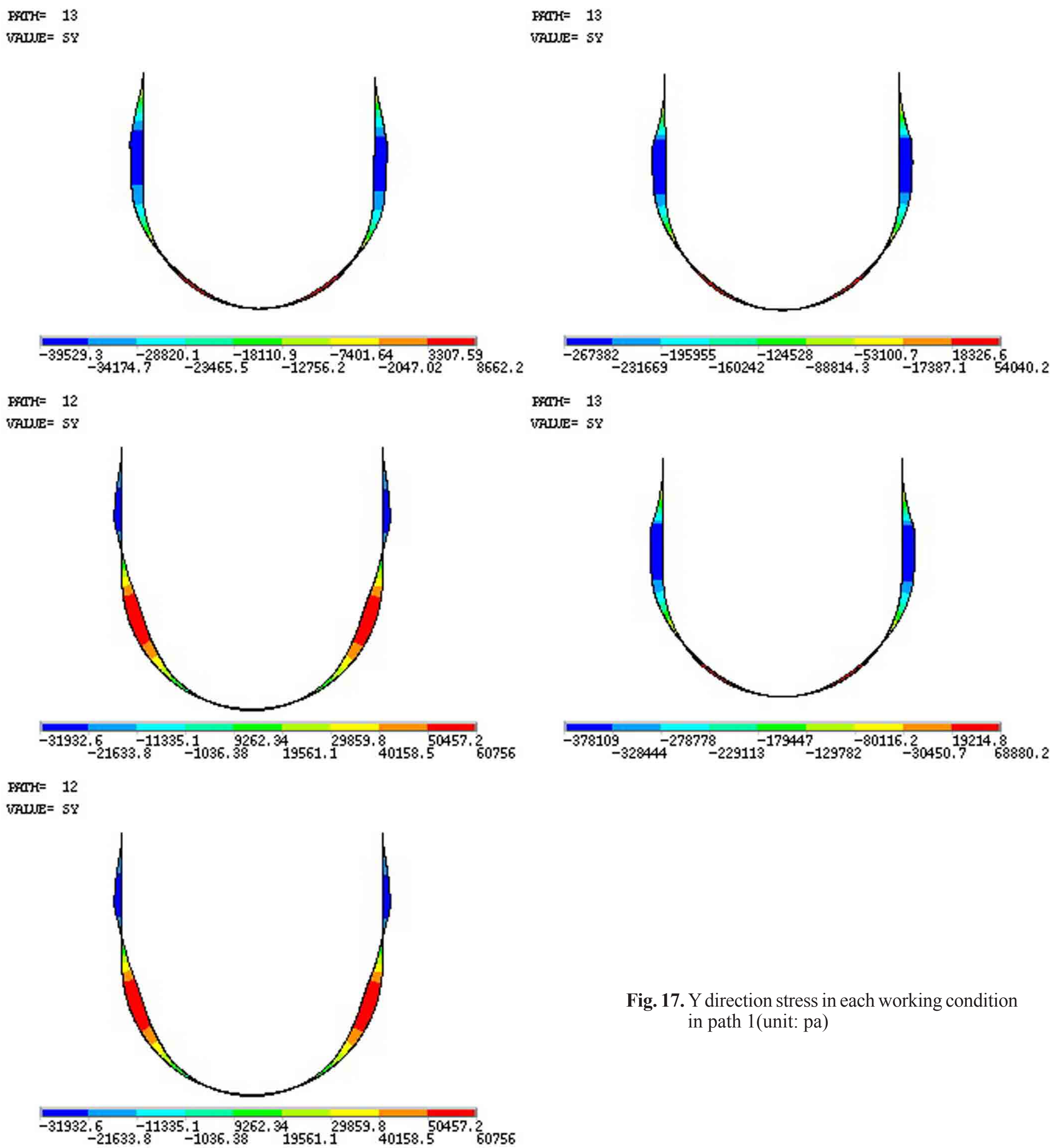

Fig. 17. Y direction stress in each working condition in path 1(unit: pa)

deformation of the whole structure and can guide the design of the aqueduct and the configuration of the steel bar.

The analysis of the results of the above displacement is as follows:

The above results can be seen that the displacement of each direction is within the allowable range and meets the requirements of the engineering design. From the above calculation results, it can be seen that the displacement of the slot is the largest in the

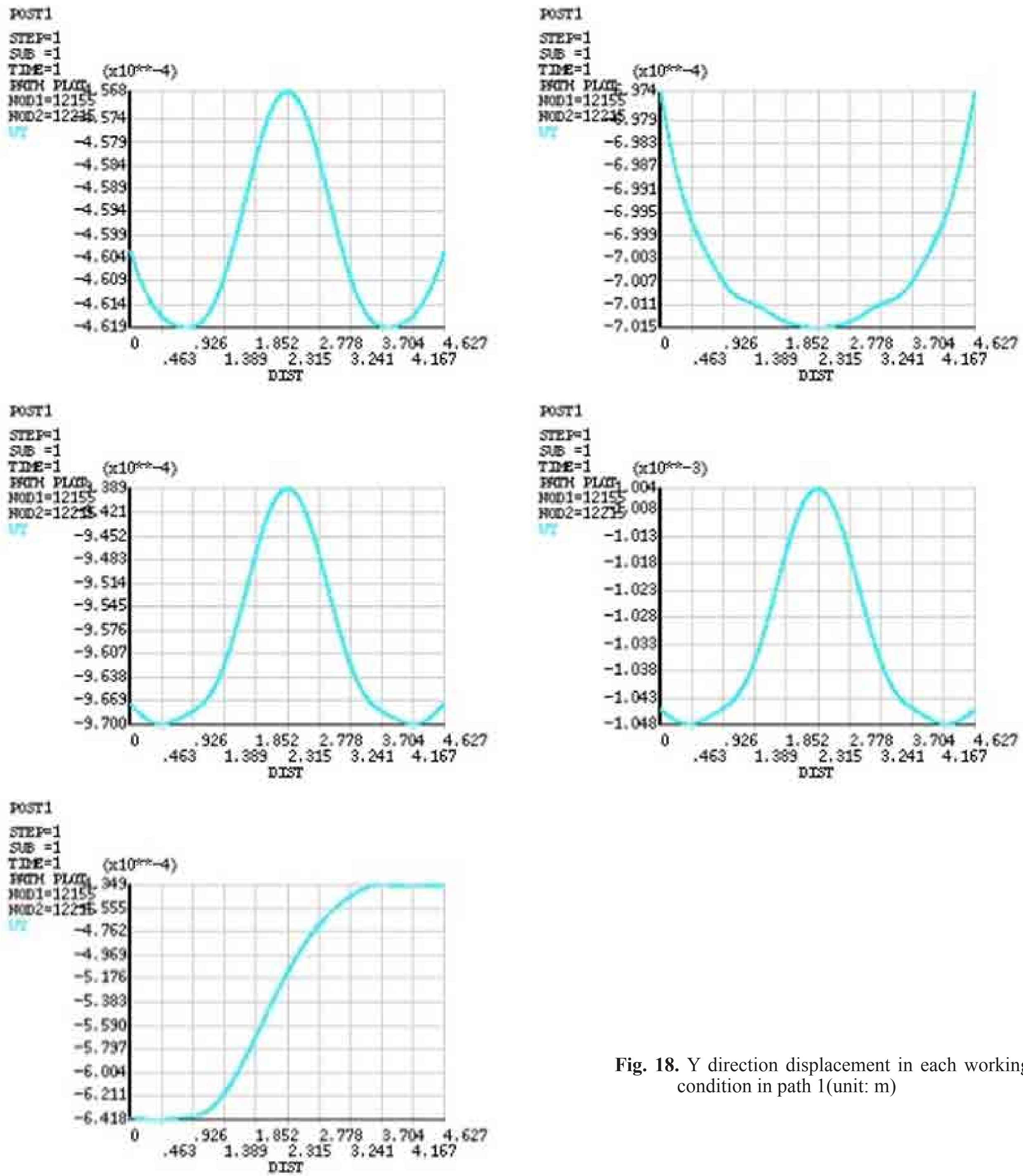

Fig. 18. Y direction displacement in each working condition in path 1(unit: m)

middle. More attention should be paid to dangerous sections, especially when excess water exceeds the designed water level. The above results can guide the configuration of steel bars in the aqueduct, as shown in **Fig. 19**.

Path 3

Results and analysis of stress calculation in Y direction in path 3

The following is the result of stress calculation:

The stress situation of the first four types of working

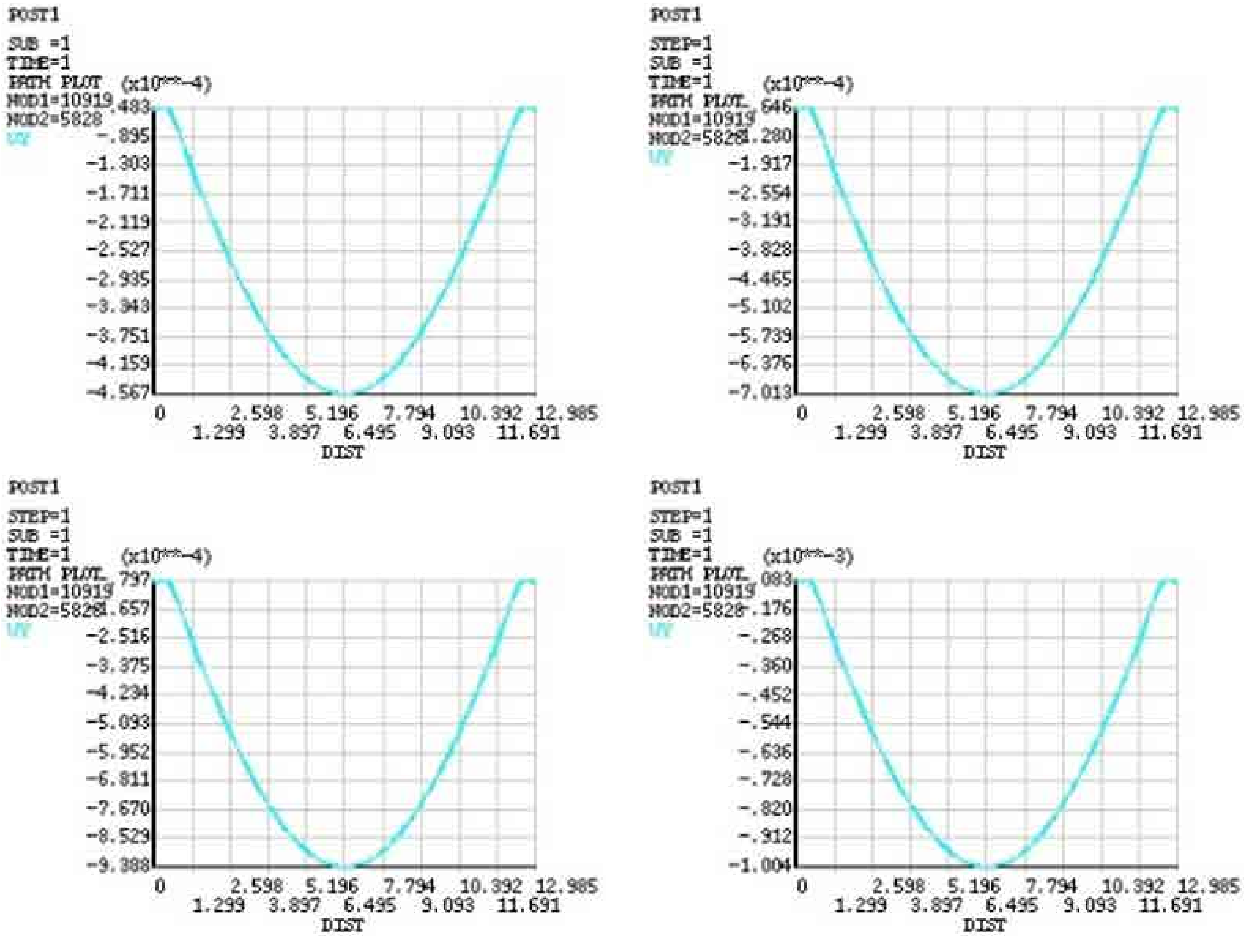

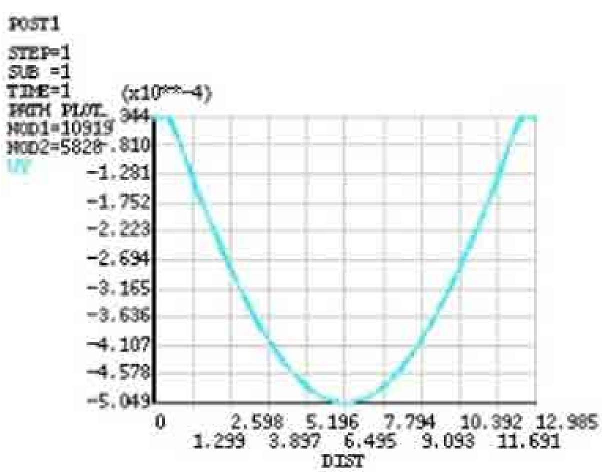

Fig. 19. Y direction displacement in each working condition in path 2(unit: m)

conditions is the same, the lower tension and the maximum tensile stress occur on the U type side wall, as shown in **Fig. 20**.

Results and analysis of Y direction displacement calculation in path 3

The following is the result of displacement calculation:

The displacement of the diagram meets the design requirements. The displacement of the middle section is the greatest, as shown in **Fig. 21**. In combination with the above calculation, the shear stress is relatively small compared to the positive stress, and the stress of the five conditions is compared and analyzed in **Table I** below.

Combined with the above calculation results, we can draw the following conclusions:

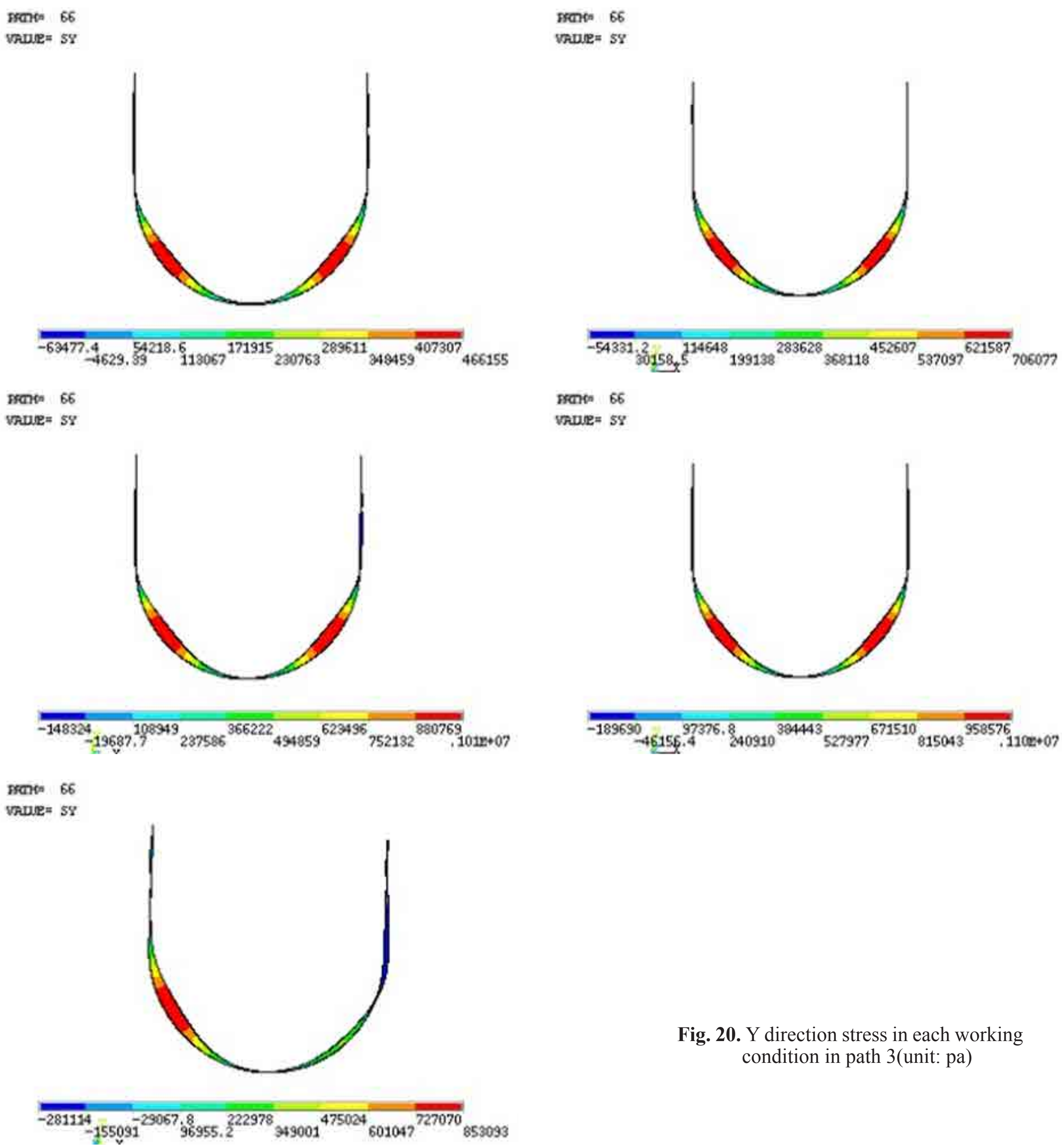

Fig. 20. Y direction stress in each working condition in path 3(unit: pa)

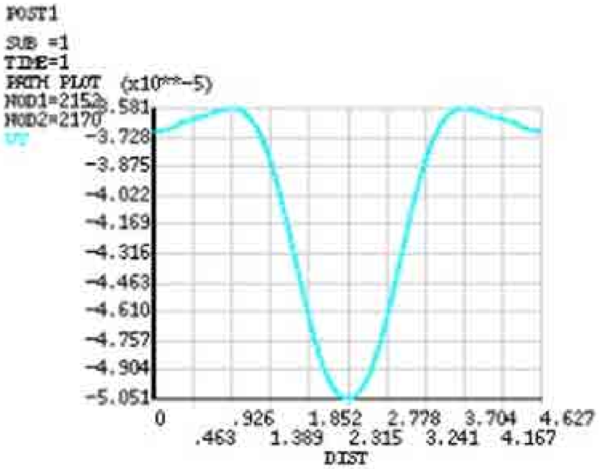

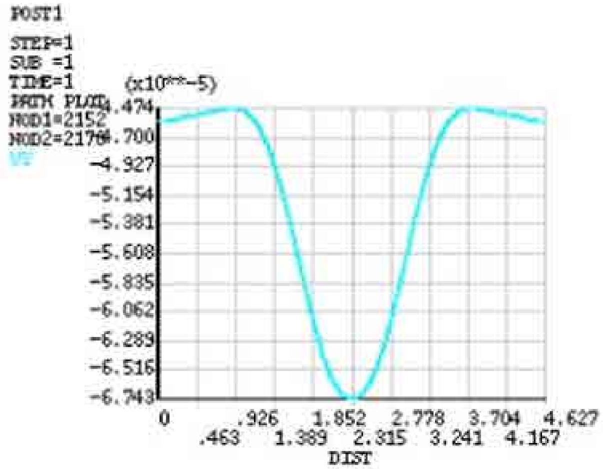

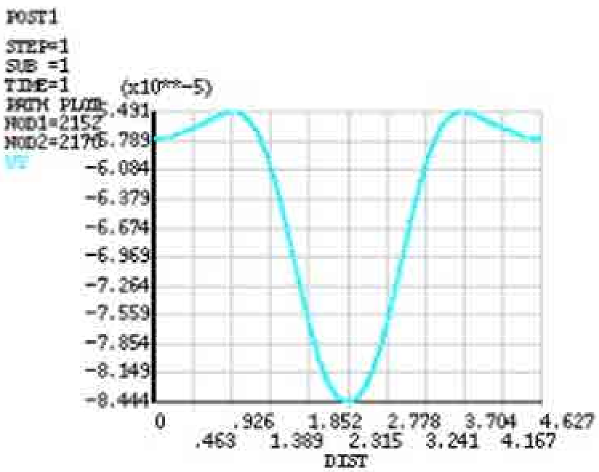

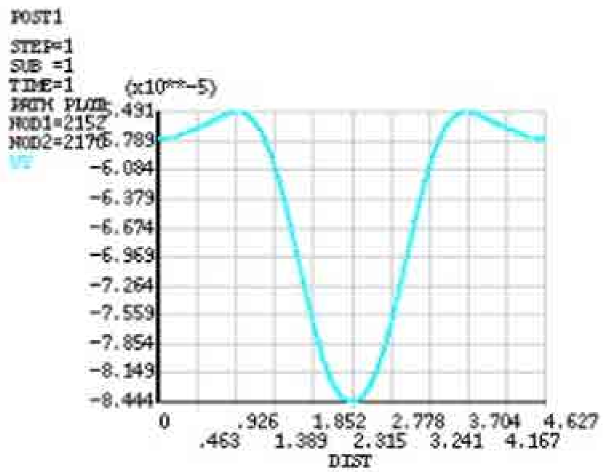

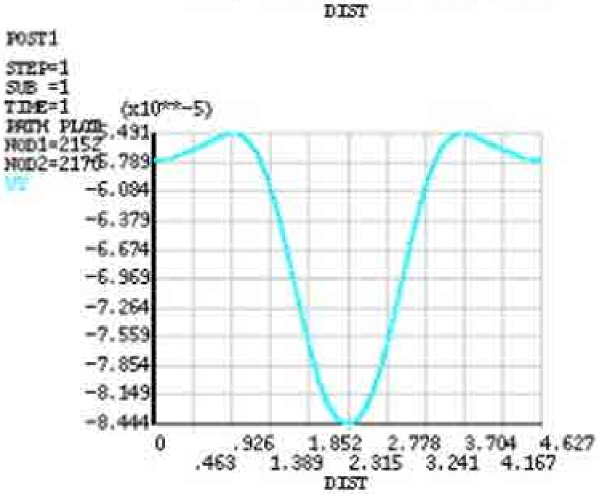

Fig. 21. Y direction displacement in each working condition in path3(unit: m)

TABLE I. THE AGGREGATE TABLE OF MAXIMUM STRESS AND DISPLACEMENT

Working Conditions	σ /Mpa	σ_y/Mpa	x directional displacement /m	y directional displacement /m	z directional displacement /m
1	0.747	0.765	0.164E-04	0.328E-04	0.981E-04
2	1.17	1.19	0.223E-04	0.400E-04	0.152E-03
3	1.56	1.65	0.480E-04	0.471E-04	0.212E-03
4	1.67	1.79	0.575E-04	0.491E-04	0.230E-03
5	1.26	1.09	0.64E-05	0.149E-05	0.129E-03

At the five working conditions, the maximum stress occurs at the middle and lower part of the slot and, all the maximum stress appears at the hinge on aqueduct ends. Under the action of gravity only, the maximum displacement of X direction occurs on both sides of the aqueduct near the end; at half water level, occurs in aqueduct body side walls; in the designed depth occurred in the middle aqueduct in the side wall; at bank full water it occurred in the lower part of the side wall; in fifth conditions it occurs in the slot end and near the end of the aqueduct. This result is related to the shape of the arc body of the U type aqueduct. The maximum displacement of the Y direction occurs in the midspan, which is in accordance with the reality. The maximum displacement of the Z direction occurs at the end of the trough, and the direction of the flow is in accordance with the actual situation.

CONCLUSIONS

Combined with the above calculation results, we can draw the following conclusions:

Under various loads, aqueduct structures are all safe and reliable, though the local stress concentration is more obvious, but it does not affect the normal operation of aqueducts. According to the calculation results of stress and displacement, it can be seen that the middle section of the tank is more dangerous. It is basically safe and reliable to use the pseudo static analysis method for seismic design in the analysis of earthquake action in this study. The weight of the water body has great influence on the stress and deformation of the structure and should be paid attention to. The end of the trough is easy to produce stress concentration and the force is more complex, so it should be analyzed and paid more attention to. The shear stress is smaller than the normal stress and cannot be considered in the analysis.

During the operation period, the maintenance of the structure near the support must be strengthened so as to prevent the damage caused by the excessive stress concentration and the excessive shear stress. The tensile stress in the span is large, and the concrete crack is easy to occur. It should be paid more attention to the neutral formwork and concrete pouring.

ACKNOWLEDGMENTS

This paper is based upon a research project supported by China Postdoctoral Science Foundation(CPSF) under grant No.2017M612227 and the Nature Science Foundation of China under grant Nos.41602287 and 51578408, The authors greatly appreciate the generous support of the CPSF and NSFC.

REFERENCES

Basheer A.O., Hanafiah M.M. and Abdulhasan M.J. (2017). A Study on Water Quality from Langat River, Selangor. Acta Scientifica Malaysia. 1(2), 01-04.

Elkafrawy F., Reda I., Elsirafy M., Gawad M.S.A., Elnaggar A. and Razek A.A.K.A. (2017). Three-Dimensional Constructive Interference in Steady State Sequences and Phase-Contrast Magnetic Resonance Imaging of Arrested Hydrocephalus. World Neurosurgery. 98, 296-302.

Erdmann W., Kelletat D. and Kuckuck M. (2017). Boulder Ridges and Washover Features in Galway Bay, Western Ireland. Journal of Coastal Research, 33 (5), 997-1021. DOI: 10.2112/JCOASTRES-D-16-00184.1.

Guangmin L., Ji R.D. and Peak G. (2007). Simulation analysis and application of prestressed steel strand. Water conservancy science and technology and economy. (10), 726-728.

Haut B. and Viviers D. (2006). Analysis of the water supply system of the city of Apamea, using Computational Fluid Dynamics. Hydraulic system in the north-eastern area of the city, in the Byzantine period. Journal of Archaeological Science. 34 (3), 415-427 .

Huang T., Li H.F., Zhang G.X., Zhao L.N., Shang F., Zhu X.M., Li D.L. and Feng S.K. (2016). Detection of Insite and Cause Analysis of Splitting Cracks of Vertical Wall for Large-scale three-direction Pre-Stressed Aqueduct. 2016 5th International Conference on Civil, Architectural and Hydraulic Engineering (ICCAHE).

Hui X. (2017). Reliability analysis of prestressed aqueduct based on ANSYS Monte Carlo method. Sichuan building materials. 43 (12), 173-174.

Ji D. (2012). Finite Element Simulation Analysis of Qiaoli Reinforced Concrete U-shaped Aqueduct. 2nd International Conference on Electronic and Mechanical Engineering and Information Technology.

Ji D. (2013). Study on finite element analysis of mortar brick rectangular-sectioned aqueduct. Conference: 2013 2nd International Symposium on Instrumentation & Measurement, Sensor Network and Automation (IMSNA).
DOI: 10.1109/IMSNA.2013.6742815.

Ji D. (2013). Three-dimensional finite element analysis for U-shaped aqueduct of Xier river. Instrumentation and Measurement, Sensor Network and Automation (IMSNA), 2013 2nd International Symposium.
DOI: 10.1109/IMSNA.2013.6743279

Jingyao P. (2013). Through analysis of Taiyuan University of Technology arch aqueduct three-dimensional finite element seismic.

Khan A.M., Yusoff I., Abu Bakar N.K., Abu Bakar A.F., Alias Y. and Mispan M.S. (2017). Accumulation, Uptake and Bioavailability of Rare Earth Elements (Rees) In Soil Grown Plants from Ex-Mining Area In Perak, Malaysia. Applied Ecology and Environmental Research. 15 (3), 117-133.

Kumruzzaman M. and Sarker A. (2017). Water requirements for various crops and impact of irrigation in barind area. Malaysian Journal of Sustainable Agriculture. 1(1), 04-07.

Lijie L. and Feng Y. (2018). A Study on The Rhythm and Respiratory Characteristics of Zhuang Language. Acta Scientifica Malaysia. 2(1), 26-28.

Navy Y. (2011). Seismic analysis of large multi slot tank type aqueduct. Hebei University of Engineering.

Razali A., Herman H.P. and Zulkifly A.H. (2017). Noise Exposure During Orthopaedics Surgery. Science Heritage Journal. 1(2), 12-13.

Rehman R., Khan A., Rashid H. and Nasir A. (2017). Performance Evaluation of Fly Ash and Red Brick Dust for Recovery of Chromium from Tannery Wastewater by Adsorption Method. Earth Science Pakistan. 1(1), 21-24.

Strzelecki P. and Sempruch J. (2016). Experimental Method for Plotting S-N Curve with A Small Number of Specimens. Polish Maritime Research. 23 (4), 129-137.

Toum G.A.E., Yassin M.I., Dagash, and Mahagoub S.A. (2018). Nitrogen Use Efficiency of Three Maize (Zea Mays L.) Cultivars. Malaysian Journal of Sustainable Agriculture. 2(1), 12-14.

Trivedi A.K., Verma S.K. and Tyagi R.K. (2018). Phenophysiological evaluation of finger millet germplasm of Central Himalayan Region. Journal of Environmental Biology. 39 (1), 31-36.
DOI: 10.22438/jeb/39/1/MRN-502.

Valeti B., Chaudhuri S.R. and Raychowdhury P. (2016). Seismic response of an elevated aqueduct considering hydrodynamic and soil-structure interactions. International Journal of Advanced Structural Engineering (IJASE). 8 (1), 53–71.

Wahab W.A. and Adzmi A.N. (2017). The Investigation of Cytotoxic Effect of Cinnamomum Zeylanicum Extracts on Human Breast Cancer Cell Line (Mcf-7). Science Heritage Journal. 1(2), 21-26.

Wang M., Zhang D.Q., Su J., Dong J.W. and Tan S.K. (2018). Assessing hydrological effects and performance of low impact development practices based on future scenarios modeling. Journal of Cleaner Production. 179, 12-23. DOI: 10.1016/j.jclepro.2018.01.096.

Yang A., Han Y., Li S., Xing H., Pan Y. and Liu W. (2017). Synthesis and comparison of photocatalytic properties for Bi2WO6 nanofibers and hierarchical microspheres. Journal of Alloys and Compounds. 695, 915-921.
DOI: 10.1016/j.jallcom.2016.10.188.

Yanhu L. (2012). Pile foundation beam multi-lateral wall prestressed aqueduct system reliability optimization design based on. of Hebei University of Engineering.

Yasin H. and Usman M. (2017). Site investigation of open dumping site of Municipal Solid Waste in Faisalabad. Earth Science Pakistan. 1(1), 25-27.

Yasin H., Usman M., Rashid H., Nasir A., Sarwar A. and Randhawa I.A. (2017). Guidelines for Environmental Impact Assessment of JHAL flyover and underpass project in Faisalabad. Geology, Ecology, and Landscapes. 1(3), 205-212.

Yun G., Williams S. and Wenbin D. (2018). Integrating Two-Stage Up-Flow Anaerobic Sludge Blanket with A Single-Stage Aerobic Packed-Bed Reactorfor Raw Palm Oil Mill Effluent Treatment. Malaysian Journal of Sustainable Agriculture. 2(1), 15-18.

Zhang B.O. and Li S.B. (2011). Cine-PC MR in assessment of cerebrospinal fluid velocity in the aqueduct of the midbrain correlated with intracranial pressure Initial study. Medical Hypotheses. 78 (2), 227-230.

Zhao H., Huang D., Wang P. and Pan W. (2011). The numerical analysis of huge rectangle aqueduct under quick cooling. Remote Sensing. Environment and Transportation Engineering (RSETE), 2011 International Conference.